

phys. stat. sol. (b) 49, 589 (1972)

Subject classification: 18.4; 22

*Institute of Physics, Sofia (a),
and Solid State Physics Department, S.C.K.-C.E.N., Mol (b)*

Neutron Diffraction Study of the Magnetic Structure of Mn_3B_4

By

S. NEOV (a) and E. LEGRAND (b)

From the neutron diffraction measurements it is concluded that below the Néel temperature of 392 K the intermetallic compound Mn_3B_4 becomes antiferromagnetic. At this stage only the Mn(2c) atoms are magnetic. Below 226 K the Mn(4g) atoms also become magnetically ordered and deform the collinear antiferromagnetic structure to a spiral structure, with an angle of 157.5°, which at lower temperature gradually develops to a collinear antiferromagnetic structure again. The saturated magnetic moments are $2.92 \mu_B$ for the Mn(2c) atoms and $0.44 \mu_B$ for the Mn(4g) atoms.

Методом нейтронной дифракции установлено, что ниже $T = 392$ К магнитная структура интерметаллического соединения Mn_3B_4 антиферромагнитна. В этом состоянии только атомы Mn(2c) имеют магнитный момент. При температуре $T = 226$ К наблюдается новый магнитный переход в спиральную структуру с углом спирали $157,5^\circ$ с одновременным появлением магнитного момента у атомов Mn(4g). Начиная с температуры 150 К структура постепенно переходит в антиферромагнитную. Определены значения насыщенного магнитного момента, который для атомов Mn(2c) равен $2,92 \mu_B$ и для Mn(4g) равен $0,44 \mu_B$.

1. Introduction

The crystal structure of Mn_3B_4 has been determined by Kiessling [1]. The unit cell is orthorhombic with space group $Immm$. The bimolecular unit cell contains 14 atoms in the positions (Fig. 1)

$$2 \text{ Mn(2c)}: \left(\frac{1}{2}, \frac{1}{2}, 0; 0, 0, \frac{1}{2} \right),$$

$$4 \text{ Mn(4g)}: \pm \left(0, u, 0; \frac{1}{2}, u + \frac{1}{2}, \frac{1}{2} \right) \text{ with } u = 0.186,$$

$$4 \text{ B(4g)}: \pm \left(0, u', 0; \frac{1}{2}, u' + \frac{1}{2}, \frac{1}{2} \right) \text{ with } u' = 0.369,$$

$$4 \text{ B(4h)}: \pm \left(0, u'', \frac{1}{2}; \frac{1}{2}, u'' + \frac{1}{2}, 0 \right) \text{ with } u'' = 0.442.$$

The Mn(4g) atoms are surrounded by four other Mn atoms at a distance of 2.68 Å, two at 2.964 Å, and two at 3.038 Å. The Mn(2c) atoms have four neighbours at 2.81 Å, two at 2.964 Å, and two at 3.038 Å. The layers of Mn(2c) and Mn(4g) atoms, parallel to the ac plane, are separated by two layers of boron atoms. On the other hand there is a close and direct contact between the Mn atoms of two neighbouring Mn(4g) layers. The complexity of the crystal structure must lead to complex magnetic interactions between the manganese atoms.

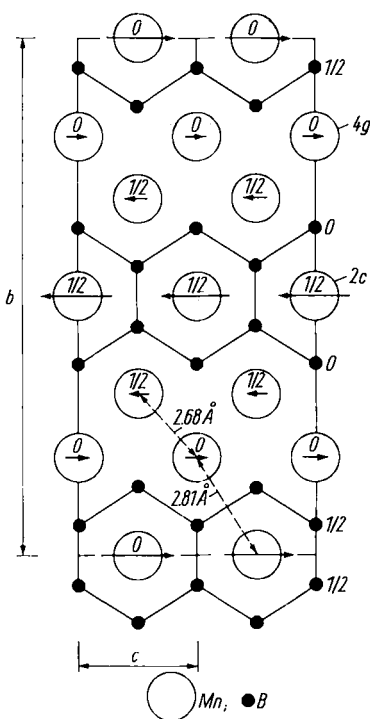


Fig. 1. Unit cell of Mn_3B_4 . The arrows show the proposed magnetic structure at liquid helium temperature

This is indeed reflected in the results of the susceptibility measurements which have been published [2 to 4]. The first susceptibility measurements, performed on powder material [2], show a transition at 392 K from a paramagnetic to an antiferromagnetic state and a second anomaly in the χ -T curve at 226 K. This has been interpreted as a change from antiferromagnetic to an helicoidal or conical arrangement of the magnetic moments. On the other hand, from the behaviour of the susceptibility in the paramagnetic region, a positive Curie constant equal to 543 K is found, which indicates that strong ferromagnetic interactions should be present. Two models for the magnetic structure are proposed by these authors: one in which the Mn(4g) atoms have a magnetic moment $\mu = 2 \mu_B$ and with no moment at all at the Mn(2c) atoms; in the second model the Mn(2c) atoms are supposed to have a moment of $3 \mu_B$ and the Mn(4g) atoms a zero magnetic moment.

Hirota and Yanase [4] prefer the first model; on the other hand Kasaya et al. [3] who present results of susceptibility measurements on single crystals assume the second model; whereas Timoshchuk and Fakidov [5] support the first model, taking into account also a small magnetic moment present at the Mn(2c) atoms.

This ambiguity in the interpretation of the susceptibility measurements justifies a more profound study of the structure of Mn_3B_4 by neutron diffraction.

2. Sample Preparation

In a first series of preparations 99.95% pure Mn and 98% pure B powders were used. Seven samples were prepared in which the boron content varied between 58 and 61 at%. However, all these samples were ferromagnetic. A mass spectrometric control of the boron powder demonstrated the presence of about 1% iron, cobalt, and nickel impurities. In agreement with the conclusions of [4] and [6], the presence of a few per cent of other transition metals in Mn_3B_4 leads to a change in the magnetic structure from an antiferromagnetic to a ferromagnetic order. Afterwards only ultra pure (99.999%) boron was used. A 58.5 at% B-41.5 at% Mn mixture was compressed under a pressure of 7.5 MP/cm^2 and heated in an evacuated (10^{-3} Torr) quartz tube during 48 h at a temperature of 1150°C . The sample was controlled with a microprobe which revealed a perfect homogeneity. The ratio between B and Mn atoms was found to be 1.30 which is very close to the stoichiometric ratio 1.33. From an X-ray spectrum the unit cell dimensions were found to be $a = 3.036 \text{ \AA}$, $b = 12.842 \text{ \AA}$, and $c = 2.964 \text{ \AA}$. This is in good agreement with the data of [1].

3. Experimental Technique

Because of the high degree of absorption of thermal neutrons by boron with the natural isotopic composition (430 b for the neutron wavelength of 1.067 Å used in the experiment), a sample of only a few tenths of a millimetre thickness should be used to get a 37% transmission. To obtain a sample with a homogeneous thickness, a flat sample holder, 1.0 mm thick, with vanadium windows was constructed and the Mn_3B_4 powder was mixed with vanadium powder in the weight ratio 2:3. The experimental transmission of the sample used in the experiments was finally 27%.

In spite of the good results of the X-ray and microfocus controls, the neutron diffraction spectra still showed the presence of a small amount of MnB in the sample. MnB is known to be ferromagnetic [2] so that it cannot give rise to superstructure diffraction peaks at lower temperatures and in fact the presence of the MnB impurity did not give rise to severe difficulties.

The temperature was controlled with Au-0.03 at% Fe against chromel thermocouples at the upper and lower sides of the sample. The maximum temperature gradient in the sample was 3 K. Diffraction spectra have been taken at several temperatures between 4.2 and 460 K.

4. Experimental Results

When the calculated nuclear intensities for positions given in [1] were compared with the experimental ones, measured above the Néel temperature, significant deviations between the calculated and measured ratios of intensities were found (see also Table 1). Therefore with the aid of the six first diffraction peaks it was tried to adjust the parameters u . The best fit between the calculated and measured intensities was found for the values $u = 0.184$, $u' = 0.363$, and $u'' = 0.436$.

To normalize the measured magnetic reflections the (110) and (011) nuclear reflections were used. Among these reflections the (110) reflection is very strong, and the (011) reflection negligibly small, moreover these reflections are quite insensitive to changes in the parameter u .

For the magnitude of the scattering lengths the following values were used: $b_{Mn} = -0.36 \times 10^{-12}$ cm and $b_B = 0.54 \times 10^{-12}$ cm [7]. The magnetic form factor as measured on $MnAu_2$ has been used [8].

At liquid helium temperature superstructure lines appear in the diffraction spectra at angle values of $2\theta = 4.7^\circ$, 14.3° , and a very weak one at 22.4° . The superstructure lines could be indexed as (010), (030), and (120) magnetic reflections, because the magnetic unit cell is no longer body-centered but primitive orthorhombic. This suggests the presence of an antiferromagnetic structure with the momentum directions perpendicular to the b -axis. Both at liquid nitrogen temperature and at room temperature the measured spectra have the same general aspect, although the smaller (030) peak is badly resolved from the background at higher temperatures.

In Table 1 the calculated intensities of four different magnetic structure models are compared with the measured intensities.

In I_{cal} (1) the calculated intensities following the antiferromagnetic model of Fig. 1 are given with the following moments for the manganese atoms: $\mu(2c) = 2.92 \mu_B$ and $\mu(4g) = 0.44 \mu_B$. This model gives the best results from all models which have been tried. I_{cal} (2) and I_{cal} (3) show the calculated

Table I

<i>hkl</i>	<i>I</i> _{obs}	<i>I</i> _{cal} (1)	<i>I</i> _{cal} (2)	<i>I</i> _{cal} (3)	<i>I</i> _{cal} (4)	<i>I</i> _{cal} (5)
(010)M	229	230	195	56	107	
(020)	39	40				59
(030)M	6	7.4	15	24	22	
(040)	36	37				32
(110) (011)	189	189	189	189	189	189
(031) (130)	143	127 17				130 10
(120)M	≤3	4	7	6	5	

magnetic intensities following the models proposed by [2], with the magnetic moments $\mu(2c) = 3\mu_B$; $\mu(4g) = 0\mu_B$, and $\mu(2c) = 0\mu_B$; $\mu(4g) = 2\mu_B$, respectively.

In I_{cal} (4) the intensities calculated on an antiferromagnetic model with $\mu(2c) = 0.5\mu_B$ and $\mu(4g) = 2.2\mu_B$ are given.

Even by varying the magnitude of the magnetic moments in the last three models no good agreement could be obtained between calculated and measured intensities.

Finally attempts were made with other models based upon an antiferromagnetic orientation between neighbouring Mn(2c) and Mn(4g) planes or in which the magnetic moments were tilted out of the planes by a few degrees, but none of them could give satisfactory results.

In column I_{cal} (5) the nuclear intensities, calculated with the parameters of [1], are presented. These parameters give rise to a large discrepancy between the calculated and measured intensities for the (020) reflection.

Attempts to correct for this discrepancy, by changing the value of the scattering length of the boron atom, did not succeed; on the other hand the calculated intensity of this reflection was very sensitive to small changes in the position parameters.

From the presence in the diffraction pattern of a weak (120) magnetic reflection and the complete absence of the (021) one, it could be concluded that the magnetic moments must be oriented parallel to the *c*-axis.

Just below the anomaly at 226 K in the susceptibility curve, the (010) reflection splits into two peaks: a large one at $2\theta = 4.18^\circ$ and a five times smaller one at $2\theta = 5.35^\circ$. This configuration changes very little down to 150 K. Below this temperature both peaks again move to each other to coincide nearly completely at 120 K. Nevertheless, even at 77 K a small asymmetry at the base of the (010) reflection is visible when this peak is compared to the peak at 4.2 K. A few examples of these peaks measured at different temperatures

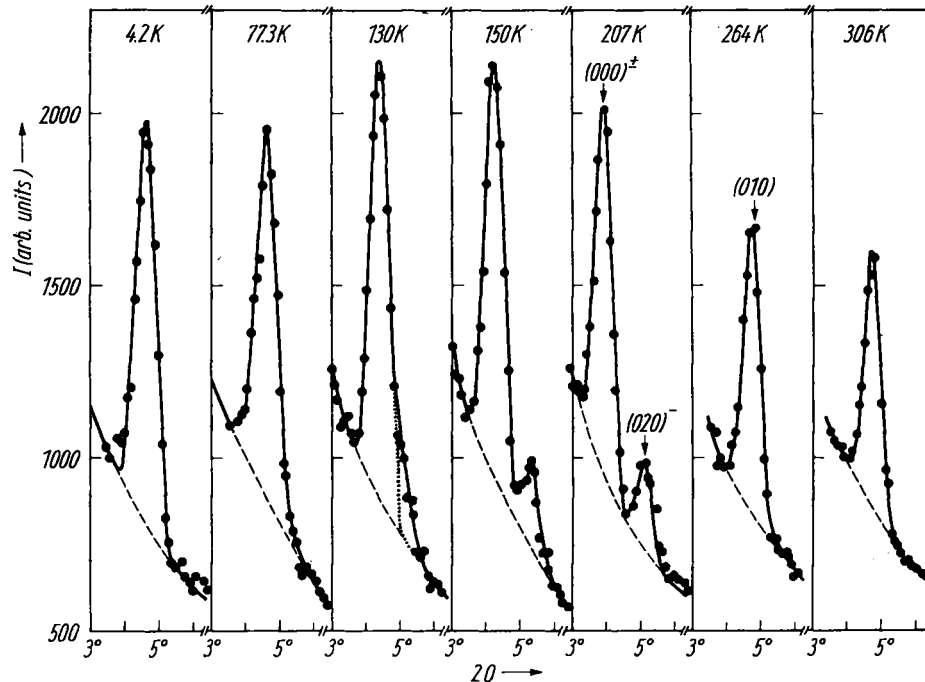


Fig. 2. Measured magnetic (010) and $(000)^{\pm}$, $(020)^{\pm}$ reflections at different temperatures

are given in Fig. 2 to illustrate the temperature dependence of the magnetic reflections.

The presence of two peaks indicates that the periodicity in the *b*-direction of the magnetic moments no longer coincides with the periodicity of the crystal unit cell. Therefore a spiral arrangement of the magnetic moments is obvious, the propagation vector \mathbf{k}_s of the spiral being along the *b*-axis. The two peaks can then be indexed as the $(000)^{\pm}$ and $(020)^{\pm}$ satellites; the small (030) peak found at 4.2 K is slightly displaced and corresponds to the $(020)^+$ satellite. It is supposed that the magnetic moments of the Mn(2c) atoms remain parallel with those of the Mn(4g) neighbours. In this case one has to consider three spiral sublattices which are in phase. After [9] the structure factor of the satellites in the case of a spiral can be calculated from

$$F_{\text{sat}} = N \left(\frac{\sqrt{1 + \cos \eta}}{2} \right) \sum_n p_n \exp(i \Phi_n) \exp(\mathbf{B}_H \cdot \mathbf{R}_n)$$

in which N is the number of unit cells, η is the angle between the scattering vector and the propagation vector of the spiral, $p_n = 0.539 \times 10^{-12} S_n f_n$ cm, S_n being the average spin value and f_n the magnetic form factor, and \mathbf{R}_n the position vector in the unit cell of the n -th magnetic atom, \mathbf{B}_H is the reciprocal lattice vector of the plane (hkl) and Φ_n is the phase angle of the n -th magnetic moment in the unit cell.

Table 2

<i>hkl</i>	<i>I</i> _{obs}	<i>I</i> _{cal} (1)	<i>I</i> _{cal} (2)	<i>I</i> _{cal} (3)	<i>I</i> _{cal} (4)	<i>I</i> _{cal} (5)
(000) [±]	190	190	360	135	240	125
(020) ⁻	38	39	55	76	61	58
(020) ⁺	(\lesssim 3)	4.4	6	8.5	7	7

In Table 2 the intensities calculated following this model for different values of the magnetic moments are compared with the intensities observed at 207 K. In the columns *I*_{cal} (2), *I*_{cal} (3), and *I*_{cal} (4) the same values for the moments are used as for the calculations presented in Table 1. In *I*_{cal} (5) the calculated intensities for a spiral structure with the same periodicity, but in which the moments of the successive manganese layers make an angle of 52.5° with each other, are given. In this case not only the calculated intensities do not correspond at all with the experimental values, but the model moreover requires satellites which are not present in the measured spectra. The best fit presented in *I*_{cal} (1) is obtained for $\mu(2c) = 2.72 \mu_B$, $\mu(4g) = 0.41 \mu_B$. It is noteworthy that these values are only slightly lower than those at 4.2 K.

From the formula $(2 \sin \theta/\lambda)^2 = (\mathbf{B}_H \pm \mathbf{k}_s)^2$ one finds a spiral angle $\varphi = \pi b |\mathbf{k}_s|$ equal to 157.5° at 207 K.

5. Discussion of the Results

A probable explanation for the change in the magnetic structure at 226 K is that this temperature is the transition temperature for the ordering of the Mn(4g) atoms. A support for this explanation can be found from Fig. 3. In this figure the dependence of the intensity of the (010) magnetic reflection is shown as a function of the temperature in the two "single-peak" temperature regions. It is difficult to connect the two groups of points, at low and high temperatures, with a Brillouin shaped curve. Moreover, the point at 4.2 K

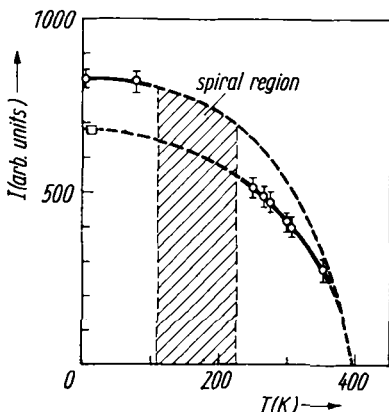


Fig. 3. Dependence of the intensity of the (010) magnetic reflection as a function of temperature

indicated with a square on the figure corresponds to the calculated magnetic intensity for a model of the magnetic structure in which the Mn(2c) atoms have a magnetic moment of $2.92 \mu_B$ which is the normal magnetic moment found for these atoms at that temperature, and the Mn(4g) atoms have a zero magnetic moment. When this point is connected by a smooth curve to the points which represent the measured intensities at high temperatures, a more common temperature dependence of the magnetic intensities is found. An other indication that the Mn(4g) atoms start to play a role in the magnetic ordering of the moments at 226 K can be found from the results of the measurements in [4]. Following these authors small amounts of cobalt and nickel impurities, added to Mn_3B_4 , should be mainly situated on the (4g) sites. These compounds are antiferromagnetic just below the Néel temperature and become ferromagnetic at about 226 K. Only when the amount of impurity atoms increases strongly, a ferromagnetic structure is also found at higher temperatures.

Both these two observations might indicate that at 226 K the Mn(4g) atoms get an ordered magnetic moment and disturb the pure antiferromagnetic order which exists at higher temperatures between the Mn(2c) atoms.

The interpretation of the diffraction measurements is compatible with the $\chi-T$ measurements on single crystals [3]. Indeed, above 226 K the susceptibility measured with an external field parallel to the crystallographic *a*-direction χ_a , and also χ_b , have higher values than χ_c . This indicates that in that temperature region the magnetic moments are directed along the *c*-axis. At 226 K there is an abrupt change in the χ_a-T and χ_c-T curves to each other and both susceptibility curves coincide below this temperature. A spiral structure, with a propagation vector in the *b*-direction, must in fact have an average susceptibility χ_a equal to χ_c . From 150 K to lower temperatures again a separation of χ_a and χ_c sets in, χ_a again becoming larger than χ_c . It is around the same temperature that the two satellite diffraction peaks move to each other to coincide almost completely at about 120 K, so that at very low temperatures a collinear antiferromagnetic structure with a magnetic moment orientation along the *c*-axis, is again probable. The value of the $\chi-T$ curve remains at any temperature above the value of χ_c , which corresponds with the model of the diffraction measurements where it is found that the magnetic moments are always perpendicular to the *b*-axis.

It would be worthwhile to perform more measurements on single crystals grown from B^{10} pure boron so that the many small magnetic intensities which should be present could be measured. We intend to perform similar diffraction measurements on the MnB_2 compound. In this structure the surrounding of the Mn atoms by boron atoms is similar as for the Mn(2c) sites in Mn_3B_4 .

Acknowledgements

One of us, S. Neov, would like to thank the I.A.E.A. organisation for the award of a fellowship which allowed him to perform these measurements at the S.C.K.-C.E.N., Mol, Belgium.

We are indebted to Prof. Dr. R. Gevers and Dr. A. van den Bosch for helpful discussions. Thanks are due to Mr. van Roy and Mr. J. Baudeweyns for their technical assistance during the measurements and Mr. F. Lafère for making the drawings.

References

- [1] R. KISSLING, *Acta chem. Scand.* **4**, 146 (1950).
- [2] H. HIROTA and A. YANASE, *J. Phys. Soc. Japan* **20**, 1596 (1965).
- [3] M. KASAYA, T. HIHARA, and Y. KÔI, *J. Phys. Soc. Japan* **30**, 286 (1971).
- [4] H. HIROTA and A. YANASE, *J. Phys. Soc. Japan* **21**, 433 (1966).
- [5] V. I. TIMOSHCHUK and I. G. FAKIDOV, *Soviet Phys. — Solid State* **13**, 85 (1971).
- [6] Y. AKIRA, T. YOSHIO, I. ATSUCHI, and H. HOZUMI, U.S. Patent No. 3424687 (1969).
- [7] G. E. BACON, *Acta cryst.* **A25**, 391 (1969).
- [8] A. HERPIN and P. MÉRIEL, *J. Phys. Radium* **22**, 337 (1961).
- [9] J. M. HASTINGS and L. M. CORLISS, *Phys. Rev.* **126**, 556 (1962).

(Received November 15, 1971)